

Spin structure function g_1 at low x : status and plans

B. Badełek^{a*}

^aPhysics Department, Uppsala University, Box 530, S - 751 21 Uppsala, Sweden, and
Institute of Experimental Physics, Warsaw University, Hoza 69, PL - 00 681 Warsaw, Poland

A brief review of measurements and expectations concerning the spin structure function g_1 of the nucleon at low values of the scaling variable x is given.

1. INTRODUCTION

The spin-dependent structure function g_1 is specially interesting at low x , i.e. at high parton densities, where new dynamical mechanisms may be revealed. Its knowledge there is needed for evaluating the spin sum rules necessary to understand the origin of nucleon spin. The behaviour of g_1 at $x \lesssim 0.001$ and in the scaling region, $Q^2 \gtrsim 1 \text{ GeV}^2$, is unknown. Spin independent structure function F_2 rises there, in agreement with QCD and contrary to the Regge model predictions. A great opportunity to explore the spin dependent phenomena in the region of low x would be through polarising the proton beam at HERA. In the fixed target experiments, low values of x are correlated with low values of Q^2 . Theoretical analysis of these results thus requires a suitable extrapolation of g_1 to the low Q^2 region where the dynamical mechanisms, like the Vector Meson Dominance (VMD), can be important. For large Q^2 the VMD contribution to g_1 vanishes as $1/Q^4$ and can usually be neglected. Moreover, the partonic contribution to g_1 which controls the structure functions in the deep inelastic domain and which scales there *modulo* logarithmic corrections, has to be suitably extended to the low Q^2 region. In the $Q^2=0$ limit g_1 should be a finite function of W^2 , free from any kinematical singularities or zeros.

2. PRESENT INFORMATION ON THE g_1 OF THE NUCLEON

2.1. Results of measurements

As a result of a large experimental effort over the years, proton and deuteron g_1 was measured for $0.00006 < x < 0.8$, cf. Fig. 1, [1] (and references therein). Direct measurements on the neutron are limited to $x \gtrsim 0.02$ (see e.g. [2]). Recent measurements by HERMES [2] are not shown in Fig. 1; those results cover the region $x \gtrsim 0.005$ and do not change the overall picture. The region of lowest x values was explored only by the SMC due to the high energy of the muon beam, the demand of a final state hadron in the analysis [3] and the implementation of a dedicated low x trigger with a calorimeter signal [4], the two latter requirements efficiently removing the dominant μe scattering background. No significant spin effects were observed there.

As seen in Fig.1 the scaling violation in $g_1(x, Q^2)$ is weak: the average Q^2 is about 10 GeV^2 for the SMC and almost an order of magnitude less for the SLAC and HERMES experiments. For the SMC data [4], $\langle x \rangle = 0.0001$ corresponds to $\langle Q^2 \rangle = 0.02 \text{ GeV}^2$; Q^2 becomes larger than 1 GeV^2 for $x \gtrsim 0.003$. At low x results on g_1 have large errors but it seems that g_1^p is positive and g_1^d and g_1^n are negative there. Statistical errors dominate in that kinematic interval. It should be noted that a direct result of all measurements is the longitudinal cross section asymmetry, $A_{||}$ which permits to extract the virtual photon – proton asymmetry, A_1 and finally, using F_2 and R , to get g_1 .

*Supported in part by the KBN grants 2 P03B 05119 and SPUB nr 621/E-78/SPUB-M/CERN/P-03/DZ298/2000

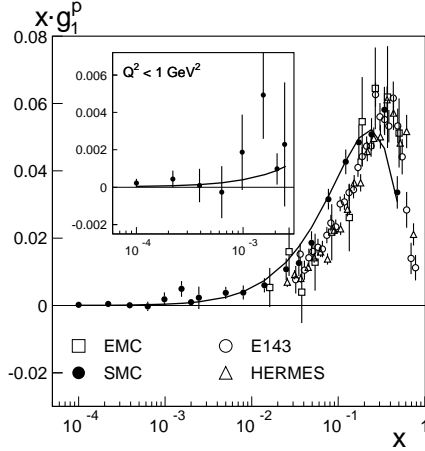


Figure 1. Summary of the xg_1^p as a function of x at the *measured* Q^2 . The insets show the SMC data for $Q^2 < 1 \text{ GeV}^2$. Errors are statistical. The curves, calculated at (x, Q^2) values of the SMC data, result of the model described in Section 2.5. Figure taken from [1].

2.2. Regge pole model expectations

The low x behaviour of g_1 for fixed Q^2 reflects the high energy behaviour of the virtual Compton scattering cross section with centre-of-mass energy squared, W^2 . This is the Regge limit of the (deep) inelastic scattering where the Regge pole exchange model should be applicable. According to this model, $g_1(x, Q^2) \sim x^{-\alpha}$ for $x \rightarrow 0$ and fixed Q^2 , where α is the intercept of the Regge trajectory, here corresponding to axial vector mesons. It is expected that $\alpha \sim 0$ for both $I = 0$ and $I = 1$ trajectories, [5]. This behaviour of g_1 should go smoothly to the $W^{2\alpha}$ dependence for $Q^2 \rightarrow 0$. It is also expected that the flavour singlet part of the g_1 should have a similar low x behaviour as the nonsinglet one. Regge model predictions for g_1 become unstable against the QCD evolution which generates more singular behaviour of g_1 than that given by $x^{-\alpha}$.

Other predictions based on the Regge model are: $g_1 \sim \ln x$, [6] and $g_1 \sim 2 \ln(1/x) - 1$, [7]. A perverse behaviour, $g_1 \sim 1/(x \ln^2 x)$, recalled in [6], is not valid for g_1 , [8].

The Regge model prediction, $g_1 \sim x^0$, has in the past often been used to obtain the $x \rightarrow 0$ extrapolation of g_1 (see Fig. 2) required to extract its first moments (cf. [9] and references therein).

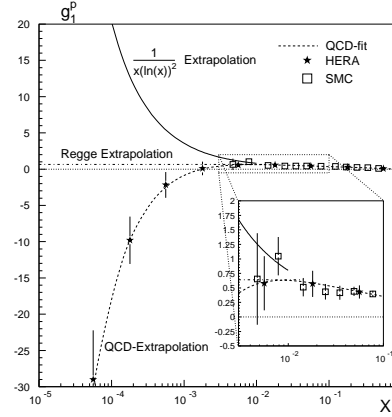


Figure 2. Three scenarios of the possible behaviour of g_1^p at low x [17].

The low x data of the SMC [4] include the kinematic region where $W^2 = (p + q)^2$ is high, $W^2 \gtrsim 100 \text{ GeV}^2$, and $W^2 \ll Q^2$. Thus the Regge model should be applicable there. However for those data W^2 changes very little: from about 100 GeV^2 at $x = 0.1$ to about 220 GeV^2 at $x = 0.0001$, contrary to a strong change of Q^2 : from about 20 GeV^2 to about 0.01 GeV^2 respectively. Thus those data cannot test the Regge behaviour of g_1 through the x dependence of the latter.

2.3. QCD fit to the world data on g_1^N

Next-to-leading (NLO) order QCD analyses of the Q^2 dependence of g_1 had been performed on the g_1 data [9–11] and have indicated a large contribution of gluon polarisation to the proton spin albeit determined with very large errors.

Extrapolations of QCD fit results to the unmeasured low x region give all three structure functions, g_1^p , g_1^d and g_1^n negative (g_1^p becomes such below the lowest x data point used in the fit), due to a large negative singlet contribution.

It should be stressed that the g_1 results for x values below these of the data do not influence the results of the fit. Thus there is no reason to expect that the partons at very low x behave as those in the measured (larger x) region. Nevertheless the low x QCD extrapolations are presently being used to get the $x \rightarrow 0$ extrapolation of g_1 [9], necessary to evaluate its first moments. They strongly disagree with the Regge asymptotic form, cf. Fig. 2.

2.4. $\ln^2(1/x)$ corrections to g_1

The small x behaviour of $g_1(x, Q^2)$ is controlled by the double logarithmic $\ln^2(1/x)$ contributions, i.e. by those terms of the perturbative expansion which correspond to the powers of $\ln^2(1/x)$ at each order of the expansion [12]. The $\ln^2(1/x)$ effects go beyond the standard (i.e. $\ln Q^2$) LO (and NLO) QCD evolution. It is convenient to resum these terms using the unintegrated (spin-dependent) parton distributions. The resulting integrated parton distributions contain nonperturbative parts, $\Delta p_j^0(x)$, corresponding to low transverse momenta of partons, to be parametrised semiphenomenologically.

A complete formalism incorporating the LO Altarelli-Parisi evolution and the $\ln^2(1/x)$ resummation at low x has been built for g_1^p [13,14]. It has been shown that the nonsinglet part of g_1 is dominated by ladder diagrams while a contribution of the nonladder bremsstrahlung diagrams is important for the singlet part. Results are presented in Fig. 3; small x effects suppress the very strong x dependence of g_1 resulting from pure Altarelli-Parisi evolution.

Even if the $\ln^2(1/x)$ effects are not important in the x range of the fixed target experiments they significantly affect g_1 in the low x region which may be probed at the polarised HERA.

2.5. Nonperturbative effects in g_1

At the low x , low Q^2 region, g_1 was represented by [1]:

$$g_1(x, Q^2) = g_1^{VMD}(x, Q^2) + g_1^{part}(x, Q^2) \quad (1)$$

The partonic contribution, g_1^{part} is at low x controlled by the $\ln^2(1/x)$ terms resummed using unintegrated parton distributions, cf. section 2.4. This formalism is very suitable for extrapolating

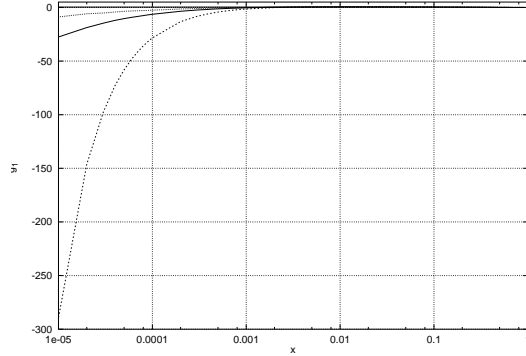


Figure 3. $g_1^p(x, Q^2)$ at $Q^2=10$ GeV² after including the $\ln^2(1/x)$ corrections. A thick solid line corresponds to full calculations, a dashed one – only the ladder $\ln^2(1/x)$ resummation with LO Altarelli-Parisi evolution, a dotted one – pure LO Altarelli-Parisi evolution and a thin solid line – the nonperturbative input to g_1 [14].

g_1 to the region of low Q^2 at fixed W^2 . Results for $g_1^{part}(x, Q^2)$ are shown as a curve in Fig.1. The VMD contribution, $g_1^{VMD}(x, Q^2)$, was taken as:

$$g_1^{VMD}(x, Q^2) = \frac{pq}{4\pi} \sum_{v=\rho,\omega,\phi} \frac{m_v^4 \Delta\sigma_v(W^2)}{\gamma_v^2(Q^2 + m_v^2)^2} \quad (2)$$

where γ_v^2 are determined from the leptonic widths of the vector mesons and m_v is the mass of the vector meson v . Unknown vector meson – nucleon cross sections $\Delta\sigma_v = (\sigma_{1/2} - \sigma_{3/2})/2$ (subscripts refer to the projections of the total spin on the vector meson momentum) were taken proportional (with a proportionality coefficient C) to the appropriate combinations of the nonperturbative contributions $\Delta p_j^0(x)$ to the polarised quark and antiquark distributions. The $\Delta p_j^0(x)$ behave as x^0 for $x \rightarrow 0$. As a result the cross sections $\Delta\sigma_v$ behave as $1/W^2$ at large W^2 that corresponds to zero intercepts of the appropriate Regge trajectories. Exact x dependence of $\Delta p_j^0(x)$ was included.

The statistical accuracy of the SMC data is too poor to constraint the value of the coefficient C . The SLAC E143 data [15] preferred a small negative value of C which is consistent with the results

of the phenomenological analysis of the sum rules [16]. Similar analysis of the neutron and deuteron spin structure functions was inconclusive.

3. g_1 AT FUTURE COLLIDERS

3.1. g_1^p

Presently the form of the $x \rightarrow 0$ extrapolation of the g_1 provides the largest error on its first moment: the contribution from the unmeasured low x region amounts from about 2 to 10% of the integral in the measured range, depending whether the Regge model or the QCD is used for the extrapolation (cf. [9] and references therein). An empirical insight into the validity of different low x mechanisms would be possible through polarising the proton beam at HERA. This would extend the measured region of x down to approximately 0.000 06 at $Q^2 \gtrsim 1 \text{ GeV}^2$.

Polarised ep (eA) colliders (HERA, EIC) will also have a potential to explore the transition between the photoproduction and scaling region, $0 < Q^2 \lesssim 1 \text{ GeV}^2$ [18,19]. Photoproduction measurements would constraint the spin dependent Regge model and Regge contribution to the Drell-Hearn-Gerasimov sum rule. Measurements in the transition region would impose new limits on g_1 models containing both perturbative and nonperturbative components.

3.2. g_1^γ

Spin dependent structure function of the photon, g_1^γ , can in principle become accessible in the future linear e^+e^- or $e\gamma$ linear colliders, [20]. The latter mode would be particularly suitable for probing the photon structure at low values of x . The $g_1^\gamma(x, Q^2)$ has been analysed [21] within the formalism being an extension of that developed for the g_1^p , [14]. It was found that e.g. different scenarios for the nonperturbative spin dependent gluon content of the photon give significantly different values of g_1^γ at $x \sim 10^{-5}$.

4. OUTLOOK

The spin dependent structure function g_1 at low x is both fascinating in itself and necessary for understanding the origin of the proton spin. Future colliders, HERA and EIC (and $e\gamma$ one for

the g_1^γ) would give us a great opportunity to explore it.

REFERENCES

1. B. Badelek, J. Kiryluk and J. Kwieciński, Phys. Rev. D61 (1999) 014009.
2. HERMES, A. Fantoni, these proceedings.
3. SMC, B. Adeva et al., Phys. Rev. D58 (1998) 112001.
4. SMC, B. Adeva et al., Phys. Rev. D60 (1999) 072004 and erratum: ibid D62 (2000) 079902.
5. R.L. Heimann, Nucl. Phys. B64 (1973) 429.
6. F.E. Close and R.G. Roberts, Phys. Lett. B336 (1994) 257.
7. S.D. Bass and P.V. Landshoff, Phys. Lett. B336 (1994) 537.
8. J. Kuti in The Spin Structure of the Nucleon, World Scientific, Singapore, 1996; M.G. Ryskin, private communication (Durham, 1998).
9. SMC, B. Adeva et al., Phys. Rev. D58 (1998) 112002.
10. For a review of older QCD analyses of g_1 see e.g. R. Windmolders, Nucl. Phys. B (Proc. Suppl.) 79 (1999) 51.
11. J. Blümlein and H. Böttcher, DESY 01-107 (2001) and hep-ph/0107317.
12. J. Bartels, B.I. Ermolaev and M.G. Ryskin, Z. Phys. C70 (1996) 273; C72 (1996) 627.
13. B. Badelek and J. Kwieciński, Phys. Lett., B418 (1998) 229.
14. J. Kwieciński and B. Ziaja, Phys. Rev. D60 (1999) 054004.
15. E143, K. Abe et al., Phys. Rev. D58 (1998) 112003.
16. V. Burkert and B.L. Ioffe, Phys. Lett. B296 (1992) 223; B.L. Ioffe, Yad. Fiz. 60 (1997) 1866 [Phys. At. Nucl. 60 (1997) 1707].
17. A. De Roeck et al., Eur. Phys. J. C6 (1999) 121.
18. S.D. Bass and A. De Roeck, Eur. Phys. J. C18 (2001) 531.
19. A. Deshpande, these proceedings.
20. M. Stratmann, Nucl. Phys. B (Proc. Suppl.) 82 (2000) 400.
21. J. Kwieciński and B. Ziaja, Phys. Rev. D63 (2001) 054022.